

# Simple theory for spin-lattice relaxation in metallic rare earth ferromagnets

W. Hübner and K. H. Bennemann

*Institute for Theoretical Physics, Freie Universität Berlin, Arnimallee 14, D-14195 Berlin,  
Germany*

(May 26, 2018)

## Abstract

The spin-lattice relaxation time  $\tau_{SL}$  is a key quantity both for the dynamical response of ferromagnets excited by laser pulses and as the speed limit of magneto-optical recording. Extending the theory for the electron paramagnetic resonance of magnetic impurities to spin-lattice relaxation in ferromagnetic rare earths we calculate  $\tau_{SL}$  for Gd and find a value of 48 ps in very good agreement with time-resolved spin-polarized photoemission experiments. We argue that the time scale for  $\tau_{SL}$  in metals is essentially given by the spin-orbit induced magnetocrystalline anisotropy energy.

78.47.+p,75.50.Cc,79.20.Ds,75.30.Gw

arXiv:cond-mat/9508120v1 25 Aug 1995

## I. INTRODUCTION

The spin-lattice-relaxation time  $\tau_{SL}$  is a sensitive fingerprint for the strength of the dynamical coupling between the spin system and the lattice. This time is therefore of interest for the long-time spin response of magnetic materials upon pulse laser lattice excitation. In a ferromagnetic solid, this time is required to establish a new equilibrium magnetization after a sudden change of the lattice temperature. Thus,  $\tau_{SL}$  is a key quantity for magneto-optical recording, since it determines the maximum speed for magneto-optical Curie-point writing<sup>1</sup>. In their pioneering work on Gd, Vaterlaus *et al.*<sup>2</sup> were the first to measure  $\tau_{SL}$  in real-time using time-resolved spin-polarized photoemission. This experiment was performed with the pump and probe technique applying strong 10 ns laser heating pulses followed by 60 ps weak probe pulses with variable delay and yielded the result

$$\tau_{SL} = (100 \pm 80) \text{ ps} \cong 5 - 50 \text{ GHz} .$$

This corresponds to a gain by two or more orders of magnitude in speed compared to the present state of the art of data processing, which is still rapidly improving.

Up to now there exists no calculation or theoretical explanation of this result. Thus, it is the goal of this paper to provide a theoretical approach to spin-lattice relaxation in metallic rare-earth ferromagnets, which is based on rate equations and an electronic model structure. We present a theory which, despite of its simplicity, exhibits already the microscopic features of spin-lattice relaxation in these materials.

The spin-lattice relaxation time  $\tau_{SL}$  describes the time required by the spins to reach thermal equilibrium with the lattice. The lattice then operates as a heat bath if one neglects the “phonon bottleneck” thus assuming perfect coupling to the external environment via the phonons. Hereby the originally cold spins are flipped by the phonons, and spin and phonon systems approach a common thermal equilibrium. This is microscopically accomplished as follows: *The spins couple to the anisotropic fluctuations of the crystal fields produced by the phonons. This coupling is mediated by spin-orbit interaction.* During this process neither a modification of the geometrical structure nor a change of the magnetic phase (long range

order) has to take place.

A typical scenario of the processes leading to spin-lattice relaxation is a four-step process: (i) The laser beam hits the sample and creates electron-hole pair excitations within  $10^{-15}$  sec. (ii) The electronic system equilibrates at elevated temperatures by electron-electron interactions within 10 fs. Note, the lattice is not yet involved. The spin and charge dynamics at the elevated temperature may already lead to the breakdown of magnetic long range order in the case of intense fs laser pulses but not for ns heating, since the electronic system is always close to equilibrium for ns photoemission. (iii) The equilibrated electronic excitations decay via phonon cascades within  $10^{-13} \dots 10^{-12}$  s and heat up the phonon system, i. e. the lattice. (iv) The phonons and the spin system reach their common equilibrium within the spin lattice relaxation time  $\tau_{SL}$  of  $10^{-10}$  s. This is also the time which allows for the recovery of magnetism in many cases, since the electronic equilibrium temperature after step (ii) might be much larger than the Curie temperature, whereas the common equilibrium temperature reached after step (iv) for spins and phonon system is usually much lower than the electronic equilibrium temperature and may also be smaller than the Curie temperature. The characteristic *interactions* of these four processes taking place on distinct time scales are: (i)  $\mathbf{p} \cdot \mathbf{A}$ , where  $\mathbf{p}$  is the crystal momentum of the electrons and  $\mathbf{A}$  is the vector potential of the laser photons, (ii) electron-electron Coulomb interaction leading to dynamical charge and spin fluctuations, (iii) electron-phonon interaction, (iv) phonon-magnon interaction caused by *spin-orbit interaction* which we will approximate by the static magnetocrystalline anisotropy energy (see below).

The experiment by Vaterlaus *et al.* was the first to measure the time evolution of the magnetic nonequilibrium state on a *picosecond* time scale. Therefore, in this paper, we exclusively address the long-time (ps to ns) response via the lattice to compare with the above experiment.

To support the above scenario of a laser pulse causing on the ps timescale and at not too low temperatures mainly the heating up of phonons, we compare the specific heat of phonons, spins, and electrons<sup>3</sup> and find the following: The spins start to dominate the

phonons at temperatures

$$T \leq T_0 \approx 0.1 \Theta_D \tag{1}$$

for fields of about 1 Tesla (in the case of paramagnetic impurities). The electrons start to dominate the phonons at temperatures

$$T \leq T_0 \approx 0.01 \Theta_D . \tag{2}$$

Typical Debye temperatures  $\Theta_D$  in ferromagnets are 420 K (Fe), 385 K (Co), 375 K (Ni), 152 K (Gd), 186 K (Dy). (For details of these estimates see appendix A). This crude estimate shows already, that phonons are dominant at sufficiently long time scales and not too low temperatures (the experiment has been performed typically at temperatures between 30 and 300 K), whereas spins (corresponding to Coulomb-correlated electrons) and finally electrons (single-particle excitations) are going to take over for lower temperatures but also for shorter times (100 fs and shorter). Thus, it appears reasonable to focus on the phonons, since the experiment has been done on the ps to ns time scale and at low temperatures. However, it becomes immediately obvious that very interesting dynamical properties of the electrons and spins are to be expected in faster (fs) pump and probe experiments which will definitely be available in the near future. However, for this time window, the notion of spin-*lattice* relaxation makes no sense any more, since electrons rather than phonons are involved.

## II. MICROSCOPIC CALCULATION OF THE SPIN-LATTICE RELAXATION TIME $\tau_{SL}$

To calculate the spin-lattice relaxation time  $\tau_{SL}$  we start from the theoretical approaches successfully applied to electron spin resonance (ESR) more than three decades ago for magnetic impurities embedded in a nonmagnetic host lattice and adapt this treatment to the solid combining phenomenological nonequilibrium thermodynamics (kinetic theory) and microscopic equilibrium theory. Three processes (all involving phonons) contribute to spin-lattice

relaxation: The direct process (Fig. 1 (a), see appendix B), the Orbach process<sup>4</sup> (Fig. 1 (b), see appendix B), both of them being relevant only at very low temperatures, and the Raman process (Fig. 1 (c)) which we consider here: This process consists of a *spin-flip*, the *absorption* of a phonon of frequency  $\omega$ , and of the *emission* of a phonon of frequency  $\omega + \omega_0$ . The longitudinal relaxation rate  $T_1$  in this case is independent of the magnetic field<sup>5</sup> and is given by

$$\frac{1}{T_1} \sim T^7 \dots T^9. \quad (3)$$

The Raman process is a two-phonon process of higher order which essentially uses the complete phonon spectrum. This process dominates the Orbach process (and thus also the direct process, see appendix B) for

$$\frac{\Delta_1}{k_B} \geq \Theta_D, \quad (4)$$

where  $\Delta_1$  is the crystal field splitting and  $k_B$  is Boltzmann's constant. Nickel, for example, has

$$\frac{\Delta_1}{k_B} \approx 688K \gg \Theta_D \approx 375K. \quad (5)$$

Thus, for not too low temperatures, the Raman-process is dominant for the spin-lattice relaxation rate.

Therefore, in view of the experimental conditions, it appears justified to focus on *Raman* determined spin-lattice relaxation in the solid which should be valid at intermediate lattice temperatures and ps time scales. The temperature range of validity forms probably the best compromise between too large temperatures where the lattice becomes unstable (above the melting point) or magnetism breaks down (above the Curie temperature) and too low temperatures where direct and Orbach processes determine the phonon induced relaxation or the phonons become frozen. Besides, the Raman process is independent of the magnetic field.

Note that purely electronic mechanisms such as spin fluctuations in strongly correlated electronic systems mediated by nuclear spin-flips (for energy and angular momentum con-

servation) via hyperfine interaction require even longer time scales and are unimportant in this context since they do not involve the lattice.

To calculate now Raman-induced spin-lattice relaxation in ferromagnetic rare earth solids we start from the theory for spin-lattice relaxation in magnetic impurities<sup>5</sup>. First we consider the number of phonons in the volume  $V$  and energy interval  $[\delta, \delta + d\delta]$

$$\rho(\delta)d\delta = \frac{3V\delta^2 d\delta}{2\pi^2\hbar^3 v_s^3}, \quad (6)$$

where  $v_s$  is the speed of sound in the material (e. g. Gd). The thermal occupation is given by the Bose factor:

$$\bar{p}_0(\delta) = \frac{1}{e^{\frac{\delta}{k_B T}} - 1}. \quad (7)$$

For the interaction, the usual crystal field expansion up to second order in terms of the randomly fluctuating strains is used

$$H_c'' \approx \varepsilon_1 \varepsilon_2 \sum_{mn} v_n^m, \quad (8)$$

since the Raman effect is of second order (see Fig. 1(c)). The transition probability from state  $|b\rangle$  to  $|a\rangle$  is then given by

$$w_{b \rightarrow a} = \int \frac{2\pi}{\hbar} |\langle b, \bar{p}_0(\delta_1), \bar{p}_0(\delta_2) | H_c'' | a, \bar{p}_0(\delta_1) - 1, \bar{p}_0(\delta_2) + 1 \rangle|^2 \rho(\delta_2)\rho(\delta_1) d\delta_1. \quad (9)$$

Including the processes of stimulated emission, absorption, and spontaneous emission the rate equation for the change of the occupation numbers of the levels  $|b\rangle$  and  $|a\rangle$  is given by ( $\rho$  is the mass density of the solid)

$$\dot{N}_b = -N_b w_{b \rightarrow a} + N_a w_{a \rightarrow b} = -\dot{N}_a = K[-N_b \bar{p}_0(\delta) - N_b + N_a \bar{p}_0(\delta)]. \quad (10)$$

Using eqs. (8) and (9) this leads to

$$\dot{N}_b = \frac{9 \sum_{mn} |\langle a | v_n^m | b \rangle|^2}{8\rho^2 \pi^3 \hbar^7 v_s^{10}} \int [N_a \bar{p}_0(\delta_2) [\bar{p}_0(\delta_1) + 1] - N_b \bar{p}_0(\delta_1) [\bar{p}_0(\delta_2) + 1]] \delta_1^6 d\delta_1. \quad (11)$$

Here, it has been used that the square of the matrix elements of the strains  $\varepsilon$  assumes the value

$$\frac{\delta[\bar{p}_0(\delta) + 1]}{2Mv_s^2}, \quad (12)$$

where  $M$  is the crystal mass. Using the plausible assumptions

$$\delta \ll k_B T, \quad \delta \ll \delta_1 \quad (13)$$

and the abbreviations

$$n = N_a - N_b, \quad N = N_a + N_b \quad \text{and} \quad n_0 = N \tanh\left(\frac{\delta}{2k_B T}\right) \quad (14)$$

yields the kinetic equation of spin-lattice relaxation

$$\dot{n} = -\frac{1}{\tau_{SL,Raman}}(n - n_0). \quad (15)$$

The microscopic calculation of the spin-lattice relaxation rate (which is the kinetic coefficient of the rate equation) gives then the result

$$\frac{1}{\tau_{SL,Raman}} = \frac{9 \sum_{mn} |\langle a | v_n^m | b \rangle|^2}{8\rho^2 \pi^3 \hbar^7 v_s^{10}} \int_0^{k_B \Theta_D} \frac{\delta_1^6 e^{\frac{\delta_1}{k_B T}} d\delta_1}{(e^{\frac{\delta_1}{k_B T}} - 1)^2}. \quad (16)$$

Using our previous estimate for the magnetocrystalline anisotropy, which is discussed in some detail in appendix C,

$$\sum_{mn} |\langle a | v_n^m | b \rangle|^2 = |E_{anisotropy}|^2 = |735 \mu eV|^2, \quad (17)$$

this microscopic theory finally yields for the spin-lattice relaxation time in Gd a value of

$$\tau_{SL,Raman} = 48 ps. \quad (18)$$

This result is in excellent agreement with the experimental value of  $(100 \pm 80)$  ps. The main issue here is that obviously the energy scale for spin lattice relaxation is set by the *magnetocrystalline anisotropy energy*, which is of the order of  $100 \mu eV - 1 meV$  at surfaces, in thin magnetic films or in hexagonal bulk crystals, rather than by the Curie temperature or by spin-orbit coupling or by electron-phonon interaction (all being of the order of  $30 - 50 meV$ ). This energy scale comes into play, since spin-lattice relaxation originates from the coupling

of the spins to the *anisotropic* crystal field fluctuations resulting from the phonons. These fluctuations flip the spins to accommodate their thermal occupation to the lattice temperature (or to a common equilibrium spin-lattice temperature). Although magnetocrystalline anisotropy results from spin-orbit coupling, its energy scale is typically smaller at interfaces or in the bulk of noncubic three-dimensional solids by a factor of 100, since spin-orbit coupling enters to second order (see appendix C). In cubic bulk crystals the leading terms are of fourth order thus resulting in a reduction factor of 10000. This argument holds for both (i) the level shifts induced by spin-orbit coupling and (ii) the occurrence and lifting of degeneracies at the Fermi energy within a small portion of the Brillouin zone<sup>6</sup>. Our argumentation is still valid even for the particular case of Gd, where the localized *f*-shell carries most of the magnetic moment while the conduction electrons are responsible for the metallicity, since the anisotropy of the magnetic moments involves the coupling of localized and conduction electrons. The same holds for the spin-lattice relaxation.

### III. CONCLUSIONS

In this work we presented a microscopic theory for the spin-lattice relaxation time  $\tau_{SL}$  in the metallic rare earth ferromagnet Gd and found a value of 48 ps in remarkably good agreement with experiment. Although our theoretical estimate neglects all detailed features of electronic structure, phonon density of states, electronic correlations, effects of electronic temperature, and the detailed form of the transition matrix elements it already yields the correct value of  $\tau_{SL}$ . Moreover, our theory clearly demonstrates the important relationship between the static magnetocrystalline anisotropy energy and the dynamic quantity  $\tau_{SL}$ , which is essential for magneto-optic recording velocities. Furthermore, our theory yields a good starting point for a detailed electronic and nonequilibrium response theory of spin-lattice relaxation in rare earth and transition metals (involving phonon-magnon coupling, see appendix D). Thus it could overcome the restriction of previous ESR theories to localized magnetic impurity spins (e. g. in insulating garnets). For thin films and multilayers, it is of particular importance to calculate the thickness dependence of this dynamical quantity, thus



checking the range of validity of the relation of  $\tau_{SL}$  to magnetocrystalline anisotropy and to the linear and nonlinear magneto-optical Kerr-effects, which involve the complementary non-spin-flip effects of spin-orbit interaction. It is a considerable theoretical challenge to investigate phonon-magnon coupling in realistic itinerant systems. From the experimental side, additional thickness dependent and *spectroscopic* pump and probe laser experiments as well as measurements of the ferromagnetic resonance (FMR yielding collective spin-flip frequencies) are required to tackle the important and complex problem of spin-lattice relaxation in metallic ferromagnetic thin film media and to bridge the gap between magnetic resonance experiments in the frequency domain and optical real-time measurements. In particular, it will be interesting to study the temperature dependence of  $\tau_{SL}$ , thus discussing also low-temperature contributions to the relaxation originating from direct or Orbach processes.

Besides, it is of considerable interest to search for faster spin-switching mechanisms using intense fs laser pulses which may directly lead to a breakdown of magnetism via electron-electron correlations and may therefore bypass the lattice thus reducing lattice heating. It is to be expected that more interesting results will be found on the *femtosecond* time scale which is now also accessible using Ti-sapphire lasers. Upon intense laser excitation, the magnetic state may break down already within some fs without the influence of the lattice and it is recovered within  $\tau_{SL}$  which involves coupling of the spins to the lattice via *anisotropic* crystal field fluctuations. In this case, the spins are cooled by the lattice rather than heated as in the experiment by Vaterlaus *et al.*, which requires a theoretical explanation. These time scales should be optically accessible in metallic thin film media in the near future.

## ACKNOWLEDGMENT

We gratefully acknowledge stimulating discussions with Prof. K. Baberschke, Dr. P. J. Jensen, and Dr. F. Meier.

## APPENDIX A: SPECIFIC HEAT OF PHONONS, SPINS, AND ELECTRONS

In this appendix, we compare the specific heat of phonons, spins, and electrons<sup>3</sup> in order to support our approximation that, at not too low temperatures, a 10 ns laser pulse heats up mainly phonons.

The low-temperature specific heat of *phonons* at constant volume is given within the Debye model by

$$c_V = \frac{12\pi^4}{5}nk_B\left(\frac{T}{\Theta_D}\right)^3 = 234\frac{T^3}{\Theta_D}nk_B. \quad (19)$$

Here,  $\Theta_D$  denotes the Debye temperature,  $k_B$  is Boltzmann's constant, and  $n$  is the number of lattice sites per unit volume.

The specific heat of the *spins* is given by

$$c_H = \frac{1}{3}\frac{N}{V}k_B J(J+1)\left(\frac{g\mu_B H}{k_B T}\right)^2, \quad (20)$$

where  $J$  is the total angular momentum and  $g$  is the gyromagnetic ratio.

The specific heat of the *electrons* is

$$c_V = \left(\frac{\partial\mu}{\partial T}\right) = \frac{\pi^2}{3}k_B^2 T \rho(\varepsilon_F) = \frac{\pi^2}{2}\frac{k_B T}{\varepsilon_F}nk_B. \quad (21)$$

The spins start to dominate the phonons at temperatures  $T$

$$T \leq T_0 = \left(\frac{N}{N_i}\right)^{\frac{1}{5}}\left(\frac{g\mu_B H}{k_B T}\right)^{\frac{2}{5}}\Theta_D \approx 0.1 \Theta_D \quad (22)$$

for fields of about 1 Tesla and  $N_i$  paramagnetic ions. The electrons start to dominate the phonons at Temperatures  $T$

$$T \leq T_0 = 0.145\left(\frac{Z\Theta_D}{T_F}\right)^{\frac{1}{2}}\Theta_D \approx 0.01 \Theta_D, \quad (23)$$

where  $Z$  is the nominal valence. Typical Debye temperatures in ferromagnets are  $\Theta_D = 420$  K (Fe), 385 K (Co), 375 K (Ni), 152 K (Gd), 186 K (Dy). This crude estimate shows already, that, for ns laser pulses, phonons are dominant at not too low temperatures.

## APPENDIX B: DIRECT AND ORBACH PROCESSES

In this appendix, we discuss the direct and Orbach relaxation processes which may dominate the Raman contributions to spin-lattice relaxation only at very low temperatures.

a) Direct process (Fig. 1):

This process consists of a *spin-flip* and the *emission* of a phonon of frequency  $\omega_0$ . The longitudinal relaxation rate is proportional to the temperature

$$\frac{1}{T_1} \sim T. \quad (24)$$

The rate is also proportional to the number of phonons within a narrow interval  $\delta$  at the extreme low-frequency end of the phonon spectrum

$$\bar{p}_0(\delta) \approx \frac{k_B T}{\delta}. \quad (25)$$

Thus, the direct process is of importance only for very low temperatures ( $T \ll \Theta_D$ ), where the other processes become negligible. The relaxation rate for the direct process depends on the magnetic field (for magnetic impurities). It is proportional to  $H^4$  for Kramers-doublets and proportional to  $H^2$  for non-Kramers-doublets.

b) Orbach process (Fig. 2):

This process<sup>4</sup> consists of a *spin-flip*, the *absorption* of a phonon of frequency  $\frac{\Delta}{\hbar}$ , and the *emission* of a phonon of frequency  $\frac{\Delta}{\hbar} + \omega_0$ . The longitudinal relaxation rate for the Orbach process is approximately given by

$$\frac{1}{T_1} \sim e^{-\frac{\Delta_1}{k_B T}}. \quad (26)$$

This rate corresponds to two high frequency cascades and is proportional to the number of phonons in a narrow band at

$$\Delta_1 \approx \text{crystal} - \text{field splitting}$$

and does not depend on the magnetic field. The Orbach process becomes important if the relation holds:

$$\frac{\Delta_1}{k_B} < \Theta_D. \quad (27)$$

At higher temperatures, however, such as in the experiment by Vaterlaus *et al.*, the Raman process should dominate the contributions originating from both the direct and Orbach processes.

### APPENDIX C: MAGNETOCRYSTALLINE ANISOTROPY

In this appendix, we give a simple estimate of magnetocrystalline anisotropy in metals, which nevertheless contains most of the features of a complete bandstructure calculation of this quantity and already yields the correct order of magnitude. For that purpose, we consider a single, for simplicity parabolic, but spin-orbit split band (Fig. 4). Hereby we neglect the fact that parabolic bands usually represent *s* electrons which feel neither spin-orbit nor exchange interaction. In addition, we neglect the magnetic dipole-dipole coupling which favors in-plane magnetization in two dimensions and is zero in the bulk of cubic or hexagonal crystals such as Gd. It is in particular the spin-orbit induced magnetocrystalline anisotropy energy which may (but does not necessarily have to) favor a perpendicular easy axis in thin films and is therefore of interest for high-density magnetic recording (the time limit of which is related to  $\tau_{SL}$ ).

We calculate now the maximum energy gain from magnetocrystalline anisotropy in this model. This gain originates from the change of the band occupation upon spin-orbit induced lifting of the band degeneracy at the Fermi level. Electrons are transferred from one branch of the band to the other. Assuming a Brillouin sphere in three dimensions one therefore obtains an anisotropy energy of

$$E_{anisotropy} = \lambda_{s.o.} \times \frac{4\pi k_F^2 \Delta k}{\frac{4\pi}{3} k_F^3} = \lambda_{s.o.} \times \frac{3\Delta k}{k_F} \quad (3D), \quad (28)$$

where

$$\frac{\Delta k}{k_F} = \frac{1}{2} \times \frac{\bar{k}}{k_F} \quad (29)$$

is the number of states contributing to the change of the electronic occupation. For typical values of the spin-orbit coupling constant  $\lambda_{s.o.} = 70$  meV and the Fermi energy  $E_F = 10$  eV we find the result

$$E_{anisotropy} = 735 \mu eV \quad (3D). \quad (30)$$

Thus, this crude model yields already important insights in some of the microscopic features of magnetocrystalline anisotropy which are confirmed by detailed calculations<sup>6</sup>: (i) The model gives the correct order of magnitude for  $E_{anisotropy}$  in films or non-cubic bulk crystals. The actual value for Gd might be somewhat smaller in Gd but this would even improve the agreement of  $\tau_{SL}$  with experiment. (ii) The model shows that the magnetocrystalline anisotropy is smaller than the spin-orbit coupling constant by two orders of magnitude since only a relatively small portion of states close to the Fermi level may gain energy from the spin-orbit induced lifting of degeneracies. For all other states the upward and downward shifts of the lifted degeneracies cancel. (iii) The model immediately yields that the anisotropy energy resulting from the lifting of degeneracies is proportional to the *square* of spin-orbit coupling, since besides the explicit linear dependence on  $\lambda_{s.o.}$  also the portion of contributing states is linear in  $\lambda_{s.o.}$ . There is no azimuthal dependence on spin-orbit coupling in this model in remarkable agreement with the line degeneracies found in Fe monolayers<sup>6</sup>. Thus, the energy gain resulting from the *lifting of degeneracies* close to the Fermi energy is of the same order of magnitude as the magnetocrystalline anisotropy originating from *level shifts* far below  $E_F$ , which can be obtained already in nondegenerate second-order perturbation theory with respect to spin-orbit coupling. (iv) The model explains why perpendicular anisotropy may be favored in thin films: Due to the reduced coordination number in these films, narrow bands of large density of states close to the Fermi level (in ferromagnets) may occur which can gain a sufficiently large amount of magnetocrystalline anisotropy energy. (v) The anisotropy at interfaces and the nonlinear magneto-optical Kerr-Effect are closely related via spin-orbit coupling although the latter results from nonlinear optical excitations. (vi) Interface hybridization of a ferromagnet with a strong spin-orbit scatterer may yield

large anisotropies due to the reoccupation of many states close to their common Fermi level.

(vii) Spin-orbit coupling does not split exchange-split bands again. Thus, the diagonal part

$$L_z S_z \tag{31}$$

just yields contrary level shifts of spin-up and spin-down bands whereas the diagonal contribution

$$L_x S_x + L_y S_y = \frac{1}{2}(L_+ S_- + L_- S_+) \tag{32}$$

yields spin-flips. It is these spin-flips that contribute to the spin-lattice relaxation time  $\tau_{SL}$  which in this view describes the time required for adapting the (temperature dependent) magneto-crystalline anisotropy to the lattice temperature. Thus, our model yields the correct order of magnitude and a change of the direction of the magnetic moments.

## APPENDIX D: PHONON-MAGNON COUPLING

If we want to conceive a similar theory for spin-lattice relaxation in ferromagnetic transition metals such as Fe we have to notice the following important difference: In the rare earth metal Gd it is sufficient to consider the localized  $f$ -electron spins carrying the magnetic moment of  $7 \mu_B$ , which gives rise to seven possible orientations ( $m_l$  quantum numbers). Thus, Raman processes may easily take place. In the transition metal Fe, however, the  $d$  electrons are itinerant (delocalized), have to be described within the band picture, and have only two orientations (spin-up and spin-down). Therefore collective and quantized magnetic excitations (magnons) have to be allowed for the spin-lattice relaxation (Fig. 5). The transition Hamiltonian then describes the phonon-magnon coupling using boson creation and annihilation operators  $a_{\mathbf{k}}^{(\dagger)}$  for magnons and  $b_{\mathbf{k}}^{(\dagger)}$  for phonons

$$H_{ph-mag}(\mathbf{k}) = D_{\mathbf{k}}[b_{\mathbf{k}}a_{\mathbf{k}}^{\dagger} + h.c.] \quad (33)$$

with<sup>7</sup>

$$D_{\mathbf{k}} = \left[ \frac{3}{3\sqrt{2}} \frac{D}{\varepsilon} F \right] \sqrt{2S(2s-1)} \sqrt{\frac{\hbar |\mathbf{k}|}{2M\bar{v}_s}}. \quad (34)$$

Here,  $D$  is some coupling strength,  $F$  some crystal field parameter,  $S$  the spin,  $M$  the effective mass, and  $\bar{v}_s$  the averaged speed of sound.

The interaction Hamiltonian  $H_{ph-mag}(\mathbf{k})$  can then be inserted in the full phonon-magnon Hamiltonian<sup>8</sup>

$$H = \sum_{\mathbf{k}} [\omega_{\mathbf{k}}^m a_{\mathbf{k}}^{\dagger} a_{\mathbf{k}} + \omega_{\mathbf{k}}^p b_{\mathbf{k}}^{\dagger} b_{\mathbf{k}} + H_{ph-mag}(\mathbf{k})] \quad (35)$$

which is easily solved by applying the unitary transformation

$$\begin{aligned} a_{\mathbf{k}}^{(\dagger)} &= A_{\mathbf{k}}^{(\dagger)} \cos \Theta_{\mathbf{k}} + B_{\mathbf{k}}^{(\dagger)} \sin \Theta_{\mathbf{k}} \\ b_{\mathbf{k}}^{(\dagger)} &= B_{\mathbf{k}}^{(\dagger)} \cos \Theta_{\mathbf{k}} - A_{\mathbf{k}}^{(\dagger)} \sin \Theta_{\mathbf{k}} \end{aligned} \quad (36)$$

to yield

$$\begin{aligned}
\omega_A &= \omega_{\mathbf{k}}^m \cos^2 \Theta_{\mathbf{k}} + \omega_{\mathbf{k}}^p \sin^2 \Theta_{\mathbf{k}} - 2D_{\mathbf{k}} \cos \Theta_{\mathbf{k}} \sin \Theta_{\mathbf{k}} \\
\omega_A &= \omega_{\mathbf{k}}^m \cos^2 \Theta_{\mathbf{k}} + \omega_{\mathbf{k}}^p \sin^2 \Theta_{\mathbf{k}} + 2D_{\mathbf{k}} \cos \Theta_{\mathbf{k}} \sin \Theta_{\mathbf{k}}.
\end{aligned}
\tag{37}$$

$\Theta_{\mathbf{k}}$  is given by

$$\tan 2\Theta_{\mathbf{k}} = \frac{2D_{\mathbf{k}}}{\omega_{\mathbf{k}}^p - \omega_{\mathbf{k}}^m}.
\tag{38}$$

This then completes the formal solution of the phonon-magnon problem.



## REFERENCES

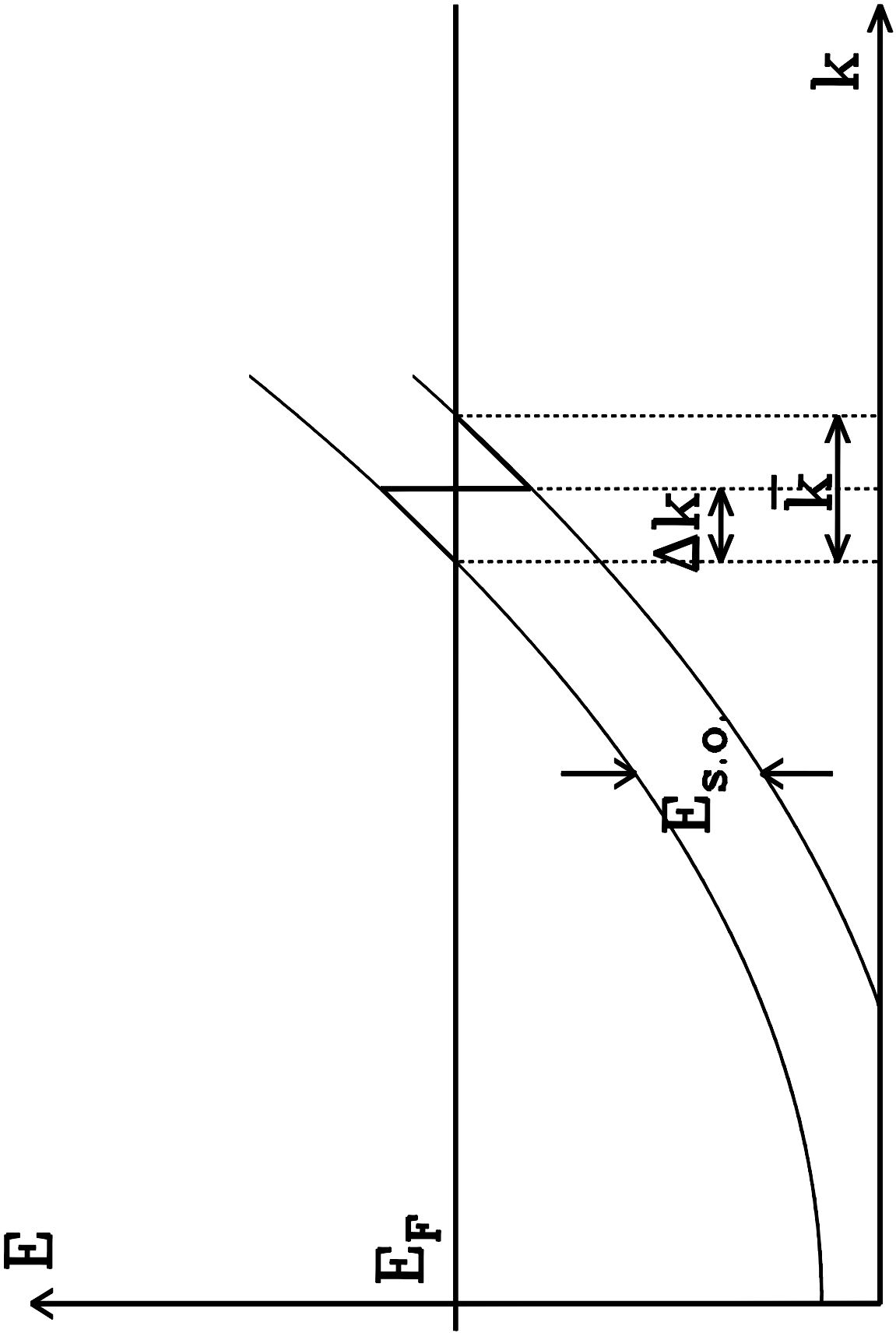
- <sup>1</sup> L. M. Falicov, D. T. Pierce, S. D. Bader, R. Gronsby, K. B. Hathaway, H. J. Hopster, D. N. Lambeth, S. S. P. Parkin, G. A. Prinz, M. B. Salamon, I. K. Schuller, and R. H. Victora, *J. Mater. Res.* **5**, 1299 (1990).
- <sup>2</sup> A. Vaterlaus, T. Beutler, and F. Meier, *Phys. Rev. Lett.* **679**, 3314 (1991).
- <sup>3</sup> N. W. Ashcroft and N. D. Mermin, *Solid State Physics* (Holt, Rinehart, and Winston, New York, 1976), pp. 464 and 669.
- <sup>4</sup> R. Orbach, *Proc. Roy. Soc. A* **264**, 458 (1961) and **264**, 485 (1961).
- <sup>5</sup> P. L. Scott and C. D. Jeffries, *Phys. Rev.* **127**, 32 (1962).
- <sup>6</sup> T. H. Moos, W. Hübner, and K. H. Bennemann (to be published).
- <sup>7</sup> U. Balucani and A. Stasch, *J. Magn. Magn. Mater.* **54-57**, 1157 (1986).
- <sup>8</sup> C. Kittel, *Quantum Theory of Solids* (John Wiley, New York, 1963), p. 74.

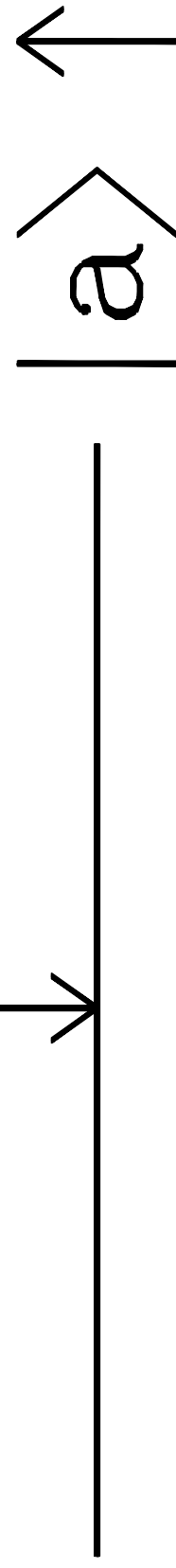
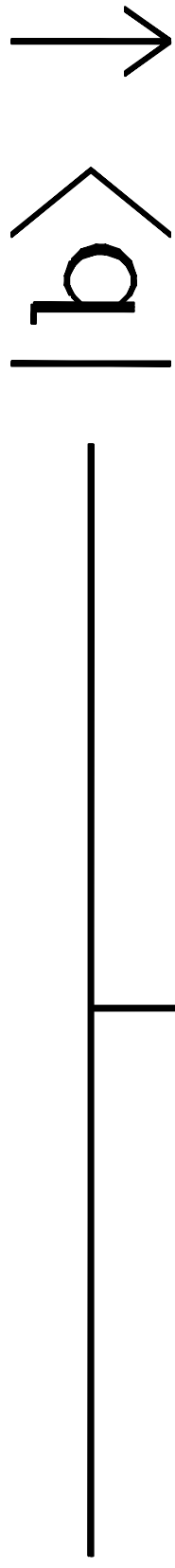
## FIGURES

FIG. 1. (a) Direct process, (b) Orbach process, and (c) Raman process.

FIG. 2. Microscopic model for magnetocrystalline anisotropy energy.

FIG. 3. Spin-lattice relaxation in transition metals.





$\hbar\omega_0$

$\delta$



